Vol. 79, No. 2

Agglutination of *Histoplasma capsulatum* by IgG Monoclonal Antibodies against Hsp60 Impacts Macrophage Effector Functions[∇]

Allan Jefferson Guimarães,[1,2] Susana Frases,[3] Bruno Pontes,[4] Mariana Duarte de Cerqueira,[5]
Marcio L. Rodrigues,[5] Nathan Bessa Viana,[4,6] Leonardo Nimrichter,[5]
and Joshua Daniel Nosanchuk[1,2]*

*Department of Medicine (Division of Infectious Diseases)[1] and Department of Microbiology and Immunology,[2] Albert Einstein College of
Medicine of Yeshiva University, Bronx, New York; Laboratório de Biotecnologia (LABIO), Instituto Nacional de Metrologia,
Normalização e Qualidade Industrial (INMETRO), Rio de Janeiro, Brazil[3]; LPO-COPEA, Instituto de Ciências Biomédicas,
Universidade Federal do Rio de Janeiro, Rio de Janeiro, Brazil[4]; Laboratório de Estudos Integrados em Biologia Microbiana,
Instituto de Microbiologia Professor Paulo de Góes, Universidade Federal do Rio de Janeiro, Rio de Janeiro,
Brazil[5]; and Instituto de Física, Universidade Federal do Rio de Janeiro, Rio de Janeiro, Brazil[6]*

Histoplasma capsulatum can efficiently survive within macrophages, facilitating *H. capsulatum* translocation from the lung into the lymphatics and bloodstream. We have recently generated monoclonal antibodies (MAbs) to an *H. capsulatum* surface-expressed heat shock protein of 60 kDa (Hsp60) that modify disease in a murine histoplasmosis model. Interestingly, the MAbs induced different degrees of yeast cell agglutination *in vitro*. In the present study, we characterized the agglutination effects of the antibodies to Hsp60 on *H. capsulatum* yeast cells by light microscopy, flow cytometry, dynamic light scattering, measuring zeta potential, and using optical tweezers. We found that immunoglobulin Gs (IgGs) to Hsp60 cause *H. capsulatum* aggregation dependent on the (i) concentration of MAbs, (ii) MAb binding constant, and (iii) IgG subclass. Furthermore, infection of macrophages using agglutinates of various sizes after incubation with different Hsp60-binding MAbs induced association to macrophages through distinct cellular receptors and differentially affected macrophage antifungal functions. Hence, the capacity of IgG MAbs to agglutinate *H. capsulatum* significantly impacted pathogenic mechanisms of *H. capsulatum* during macrophage infection, and the effect was dependent on the antibody subclass and antigen epitope.

Histoplasmosis is a cosmopolitan mycosis caused by the pathogenic fungus *Histoplasma capsulatum*. In the United States, *H. capsulatum* is endemic in the midwestern and southeastern regions (44, 45). The spectrum of disease caused by *H. capsulatum* includes asymptomatic acquisition, acute influenza-like illness, chronic cavitary pulmonary disease, and highly lethal disseminated disease. These manifestations depend mainly on the magnitude of exposure (i.e., the number of fungal particles inhaled), the immunological status of the host, and the virulence of the acquired strain, indicating that environmental, host, and fungal factors influence the manifestation of disease (9). Infection with *H. capsulatum* usually occurs via inhalation of fungal propagules that are deposited in alveoli and rapidly convert to a parasitic yeast form prior to or after ingestion by pulmonary macrophages (23). The pathogen can survive within phagolysosomes (1) of macrophages that can then act as a vehicle for fungal translocation into hilar and mediastinal lymph nodes, from which *H. capsulatum* can subsequently access the bloodstream and disseminate (45, 48).

Hsp60 (heat shock protein of 60 kDa) is the major surface ligand on *H. capsulatum* that engages macrophages via CD11b/CD18 (CR3) receptors (13, 20) for association and subsequent entry of the fungus. Phagocytosed *H. capsulatum* yeast can inhibit phagosomal-lysosomal fusion and survive within the

phagosomes of resident macrophages. The fungus avoids triggering host cell fungicidal mechanisms, including reactive oxygen metabolites and products of the nitric oxide synthase (NOS) pathway (47). However, ingestion of opsonized *H. capsulatum* can stimulate significant oxidant release (5, 47), suggesting that induction of the respiratory oxidative burst may occur upon Fc-mediated phagocytosis. Although experimental findings suggest that the protective response against histoplasmosis is mainly cellular, we have demonstrated that monoclonal antibodies (MAbs) can modify the pathogenesis of histoplasmosis to benefit the host (11, 12, 31, 32). However, the mechanisms involved in humoral protection against *H. capsulatum* yeast cells are not fully understood. Immunoglobulin M (IgM) MAbs against the histone 2B-like protein (H2B) and IgG1 and IgG2a against the Hsp60 protein reduced the *H. capsulatum* fungal burden, decreased pulmonary inflammation, and prolonged survival in a murine infection model (11, 31, 32). In contrast, an IgG2b MAb to Hsp60 was not protective (11). Protection mediated by MAbs was associated with enhanced levels of interleukin-4 (IL-4), IL-6, and gamma interferon (IFN-γ) in the lungs of infected mice. Although MAbs to H2B increased phagocytosis of yeast through a CR3-dependent process, the intracellular growth and survival of the opsonized yeast were reduced (31, 32). IgG1 and IgG2a subclass MAbs to surface Hsp60 also bound *H. capsulatum* and activated the antifungal properties of macrophages in a dose-dependent manner, as described in other pathogen-antibody models, including with antibody interactions with other fungi

* Corresponding author. Mailing address: 1300 Morris Park Avenue, Ullmann 107, Bronx, NY 10461. Phone: (718) 430-2993. Fax: (718) 430-8968. E-mail: josh.nosanchuk@einstein.yu.edu.

(11, 27) and for antibodies to pathogen heat shock proteins (21, 49). Interestingly, increased rates of phagocytosis by the IgG1 subclass MAbs was primarily via Fc receptors, whereas the IgG2a MAbs utilized both Fc and CR3 receptors to augment phagocytosis (11).

Agglutination caused by antibodies for the yeast-like fungus *Cryptococcus neoformans* has been observed (16), but the *in vitro* effects of aggregation of yeast on macrophage function remain unclear. Our prior studies with MAbs to *H. capsulatum* Hsp60 suggested that they could induce variable agglutination of yeast cells. In the present work, we have characterized the agglutination effects of the MAbs by microscopy, dynamic light scattering, flow cytometry, measuring the cellular charge, and using optical tweezers. In all experiments, we studied spontaneous formation of antigen-antibody bonds and correlated this effect with agglutination activity. We propose that characterizing the agglutination effects of antibodies can enhance our understanding of the mechanisms involved in host-pathogen interactions. Our study reveals new insights into the action of MAbs that can help us clarify the role of these molecules in immunodefense and may facilitate a rationale for the development of new therapeutics involving these reagents.

(The data provided in this paper are from a thesis to be submitted by A. J. Guimarães in partial fulfillment of the requirements for the degree of Doctor of Philosophy from the Sue Golding Graduate Division of Medical Science, Albert Einstein College of Medicine, Yeshiva University, Bronx, NY.)

MATERIALS AND METHODS

Fungal strains and MAbs. The reference strain *H. capsulatum* G217B was obtained from the American Type Culture Collection (ATCC; Rockville, Maryland). Green fluorescent protein (GFP)-expressing strain G217B (*H. capsulatum* GFP) was a kind gift from George S. Deepe (University of Cincinnati College of Medicine, Cincinnati, OH). *H. capsulatum* yeast was grown for 2 days in Ham's F-12 medium at 37°C as described previously (1). The IgG1 (11D1), IgG2a (4E12, 12D3, and 13B7) and IgG2b (7B6) MAbs to recombinant *H. capsulatum* Hsp60 were generated and quantified as described previously (11).

Murine peritoneal macrophages. Four- to eight-week-old female C57BL/6 CD11b$^{-/-}$ (strain B6.129S4-*Itgam^{tm1Myd}*/J) mice were obtained from Jackson Laboratory (Bar Harbor, MA). Animals were euthanized according to the guidelines of the Institute for Animal Studies of the Albert Einstein College of Medicine. Resident peritoneal macrophages were collected by injection of 10 ml of ice-cold Dulbecco modified Eagle medium (DMEM; Gibco, CA) into the peritoneal cavity. The cells were centrifuged and washed once with ACK lysis buffer (Lonza, MD) and twice with DMEM. Cells were suspended in complete DMEM containing 10% heat-inactivated fetal calf serum, 10% NCTC-109 medium (Sigma-Aldrich), 1% Pen-Strep, and 1% nonessential amino acids (Gibco BRL, Grand Island, NY).

Kinetics of MAb binding. Dissociation constant (K_d) values were calculated by an inhibition enzyme-linked immunosorbent assay (ELISA) on plates to which 10^5 cells/well were affixed overnight, blocked with 1% (wt/vol) bovine serum albumin diluted in phosphate-buffered saline (PBS; blocking buffer), and subjected to MAb binding as described previously (10). A second blank ELISA plate was blocked for 1 h at 37°C, and a solution of 2 μg/ml of each MAb was incubated with serial dilutions of recombinant Hsp60 (concentrations of 0.2 mg/ml to 0.195 μg/ml or 3.23 μM to 0.195 nM) at 37°C for 1 h. The contents of the wells were transferred to blocked reaction plates with adherent yeast as the antigen. After incubation at 37°C for 1 h, the plates were washed, and anti-mouse IgG conjugated with alkaline phosphatase (1:1,000 in blocking buffer) was added to the wells for 1 h at 37°C. The plates were again washed, incubated with a *p*-nitrophenyl phosphate substrate solution, and read at 405 nm. The concentration of antigen required for 50% competition was considered the K_d value.

Aggregation of *H. capsulatum* yeasts. *H. capsulatum* yeast cells were washed, suspended in PBS, and passed 10 times through a 26-gauge by 1/2-in. needle to disrupt nonspecific aggregation. Passage did not affect fungal viability, as determined by plating (data not shown). Yeast was centrifuged for 2 min at 500 rpm,

and supernatant containing single cells was decanted. The concentration of cells was determined by hematocytometer counting, and 10^6 yeast cells were added to microcentrifuge tubes containing 100, 75, 50, 25, or 12.5 μg/ml of a MAb to Hsp60, isotype control MAb, or PBS. Samples were incubated for 1 h at 37°C on a rotatory shaker and gently washed 3 times with PBS prior to use.

Bright-field microscopy and flow cytometry. Agglutination was determined by light microscopy as described previously (7), with some modifications. Briefly, the yeast was fixed in 4% formalin, stained with Grocott silver (3), and adhered to slides previously coated with poly-L-lysine (Sigma-Aldrich, St. Louis, MO). All images were taken on an Axio Imager microscope (Carl Zeiss MicroImaging, Inc., Thornwood, NY), and the area of the agglutinates was measured with ImageJ 1.39g software (National Institutes of Health [NIH], Bethesda, MD). The diameter was estimated from the area based on the circular forms of aggregates [area = ($\Pi \times d^2$)/4; Π = ratio of a circle's circumference to its diameter, d = diameter] (see Fig. 2I). Similarly, measurements were performed using GFP-labeled *H. capsulatum* cells and fluorescence microscopy to support the microscopy measurements.

Furthermore, flow cytometry was used to determine the relative diameter values of agglutinates obtained after incubation of GFP-labeled yeast cells with different concentrations of MAbs. Diameter and fluorescence intensity of agglutinates were analyzed in a FACScan flow cytometer (BD Biosciences, Franklin Lakes, NJ).

Zeta potential measurements. Yeast cells incubated with PBS or MAb 11D11 (IgG1), 12D3 (IgG2a), or 7B6 (IgG2b) or an irrelevant control were washed three times with and suspended in 20 mM KCl in lipopolysaccharide (LPS)-free water, which is the standard solution for the zeta potential analyzer (ZetaPlus; Brookhaven Instruments Corp., Holtsville, NY). Zeta potential (ζ), particle mobility, and shift frequency were analyzed to compare the zeta potentials of the different cell suspensions and agglutinates. ζ is a measurement of charge (in millivolts) defined as the potential gradient that develops at the surface of particles and the boundary of shear. It is derived from the equation $\zeta = (4\pi\eta m)/D$, where D is the dielectric constant of the medium, η is the viscosity, and m is the electrophoretic mobility of the particle in the medium.

Dynamic light scattering. Polystyrene beads (85 nm; Polysciences, Inc., Warrington, PA) were coated with a cell wall/membrane extract of *H. capsulatum* yeasts obtained as described previously (8) in order to mimic the surface composition of the yeast on the beads. Briefly, polystyrene beads were sonicated for 10 min and incubated overnight with a 100-μg/ml solution of cell wall extract diluted in carbonate buffer (0.063 M, pH 9.6). Beads were washed three times in PBS, and 10^7 beads were used in incubations with different dilutions of MAbs or controls for 1 h at 37°C. Agglutination was analyzed by quasielastic light scattering (QELS) in a 90Plus/BI-MAS multiangle particle sizing analyzer (Brookhaven Instruments), and the effective diameters and polydispersity of agglutinates were measured. Effective diameter is considered the diameter of the imaginary coaxial cylinder that intersects the surface of the thread. Polydispersity is a measure of the distribution of molecular mass in a complex mixture of polymers and indicates the distribution of individual molecular masses.

MAb-coated polystyrene beads. Polybead 3-μm carboxylate microspheres (Polysciences, Inc., Warrington, PA) were suspended in 50 mM morpholineethanesulfonic acid (MES) buffer (pH 5.2) and incubated with a 200 mg/ml solution of EDC [1-ethyl-3-(3-dymethylaminopropyl)carbodiimide hydrochloride]. After 1 h, 500 μg Avidin (Sigma-Aldrich, MO) was added, and the mixture was incubated for 1 h at room temperature (RT) with gentle mixing. Microspheres were washed with 10 mM Tris, pH 8.0, and 0.05% bovine serum albumin and stored at 4°C. MAbs were biotinylated using sulfo-NHS-Biotin (Pierce, Rockford, IL), according to the manufacturer's instructions. Avidinated microsphere beads and biotinylated antibodies were coincubated, and MAb-coated microspheres were washed with and suspended in 10 mM Tris, pH 8.0, and 0.05% bovine serum albumin.

Flow cytometry was used to estimate the surface density of antibodies bound to microspheres. For these measurements, fluorescein isothiocyanate (FITC)-labeled anti-mouse IgG (Southern Biotech, Birmingham, AL) was incubated with the MAb-coated microspheres. Unbound FITC-labeled antibodies were removed by washing, and the fluorescence was measured by flow cytometry. Additional determination was performed by fluorescent microscopy of the sphere, with fluorescence intensity measured by ImageJ.

Agglutination of MAb-coated polystyrene beads with *H. capsulatum* yeasts. To assess agglutination of antibody-coated microspheres with *H. capsulatum* yeast, the microspheres were incubated with yeast at bead/yeast ratios ranging from 10:1 to 1:1, and the aggregation effect was evaluated by flow cytometry to determine the diameters of the particles as described above. Under these conditions, the overall detachment is controlled by a multivalent process with formation of numerous interactions between the MAb microsphere and the yeast.

In particular, once the first bond is formed, other antibody-antigen pairs may be close enough to each other and form more bonds. Thus, increased antibody-antigen interactions resulted in larger agglutinates. The efficacy of agglutination was then correlated to the binding efficacy of the MAbs, as obtained by inhibition ELISA.

Optical tweezers. Optical tweezers can evaluate interaction events in single-cell experiments (38). We used optical tweezers to assess the impact of IgG subclass MAbs in the interaction between two distinct *H. capsulatum* yeast cells. For these experiments, we used opsonized *H. capsulatum* yeast cells with the nonprotective IgG2b MAb 7B6 or the protective IgG2a 12D3 and compared their impact on interactions with nonopsonized yeast cells (negative control). Briefly, 10^6 yeast cells were incubated with 75 μg/ml MAb or PBS for 1 h at 37°C and washed three times with and suspended in 200 μl of PBS. Aliquots of 100 μl were plated onto glass-bottom dishes (10-mm glass; MakTek Corporation, MA) and incubated for 2 h in order to attach the cells to the coverslip. Then, the other 100 μl of the yeast suspension was added to the same glass-bottom dish. A yeast cell in suspension was then trapped with the optical tweezers and brought directly adjacent to a second yeast cell attached to the coverslip. The interaction was allowed to occur for different times (ranging from 2 to 60 s). The microscope stage was then moved with a controlled velocity in an effort to detach the optically trapped yeast cell from the cell attached to the coverslip. The maximum optical force in these experiments was set to be in the order of 200 pN (42). If the cell-cell attachments were stronger than the maximum force, the cells remain in contact, and we considered this event a positive adhesion event. The relative adhesion was defined as the number of positive adhesion events (N) divided by the total number of attempts (N_0). The relative adhesion was measured for each time and under each experimental condition. The characteristic time was defined as the time required for 63% of the interactions to be positive in all the attempts, and it was determined based on the best fit for all the curves obtained, according to the following equation:

$$\frac{N}{N_0} = 1 - \exp\left(-\frac{t}{\tau}\right)$$

t, where exp is exponential. The error bars in the relative adhesion experiments were determined as half the difference between the maximum and minimum values at each time in 30 events performed in 3 different samples. The error bars in the characteristic time were obtained using the best curve fit to the equation shown above, weighting the data with the errors of the relative adhesion. The curve fit was performed using KaleidaGraph software (Synergy Software, Essex Junction, VT).

Fab fragments. Protective and nonprotective MAbs (12D3 and 7B6, respectively) (11) were used to generate Fab fragments to characterize the impact of these antibody components on aggregation and determine whether or not an intact antibody is required for the agglutination effect. MAb fragments were generated by treatment with immobilized papain (Pierce Scientific, Rockford, IL), according to the manufacturer's instruction. Equal molar concentrations of Fab fragments and intact MAbs were used in incubations with *H. capsulatum* yeast as described previously, and aggregation effects were evaluated by flow cytometry.

Effector functions of macrophages. The influence of *H. capsulatum* agglutination during interaction with macrophages was studied by association and growth assessment experiments. Agglutinates were generated with various concentrations of MAbs as described above, and phagocytosis and growth assessment experiments were performed as described previously (11, 32). After the incubations and the washes, the aggregates where counted again to confirm that there was an equal number of cells for each of the distinct conditions. Agglutinates were also sonicated before addition to macrophages, and they were plated on brain heart infusion (BHI) blood agar plates in order to confirm equivalence in CFU. Briefly, macrophage-like J774.16 cells were grown in 24-well cell culture polystyrene plates overnight at 37°C in 5% CO_2. Peritoneal macrophages were also extracted from CD11b$^{-/-}$ mice, and 4×10^5 macrophages were plated in a 24-well plate for 1 h at 37°C in 5% CO_2. Agglutinates obtained after incubation of GFP-labeled *H. capsulatum* yeast cells with each of the MAbs in concentrations ranging from 100 to 12.5 μg/ml were added to the macrophages, and the plates were incubated for 1 h at 37°C in 5% CO_2. All samples were processed in triplicate. After incubation, monolayers were washed with PBS, and macrophages were removed by pipetting or scraping. Cells were fixed with 4% paraformaldehyde (PF 4%) for 30 min at room temperature and then washed three times with PBS. Infected macrophages displayed fluorescent yeast, and the association index (total number of macrophages containing *H. capsulatum* adhered and/or internalized) was measured using a FACSCalibur flow cytometer (BD Biosciences), where 10,000 events were recorded. The percentage of infected

TABLE 1. Dissociation constants of MAbs obtained by inhibition ELISA

MAb	Inhibition ELISA (rHsp60) result[a]		
	B_{max}	NS	K_d
11D1 (IgG1)	−77.53	−1.055	0.080
4E12 (IgG2a)	−107	2.978	0.056
12D3 (IgG2a)	−105.4	1.610	0.043
13B7 (IgG2a)	−103.2	1.374	0.035
7B6 (IgG2b)	−83.21	1.135	0.22

[a] A correlation of the values was observed ($P = 0.045$; Pearson's $r = 0.89$). B_{max}, maximum specific binding in percentage units; NS, slope of nonspecific binding in percentage units divided by concentration; K_d, equilibrium binding constant in concentration units (μg/ml) needed to achieve half-maximum binding at equilibrium.

macrophages was obtained under each experimental condition. Additional phagocytosis experiments were performed using macrophages on which CR3 receptors or the Fc receptor were blocked by anti-mouse CD11b (integrin α-M chain, Mac-1 α-chain, and clone M1/70; Southern Biotechnologies) or anti-mouse CD 16/32 (clone 93; Southern Biotechnologies), respectively.

The influence of agglutination on the growth of intracellular yeast was also evaluated. Washed agglutinates were added to wells containing J774.16 cells and incubated for 24 h. The cultures were washed with cold PBS, and macrophages were lysed by adding sterile water. Aliquots were plated onto BHI blood agar plates (50 ml/liter of sheep red blood cells, 10 g/liter glucose, 0.1 g/liter cysteine, 1% Pen-Strep) and incubated at 37°C. The percent growth was determined by comparison of the number of CFU of *H. capsulatum* grown with macrophages and MAbs to the number of CFU of yeast grown in media alone. The dependence of growth inhibition on the yeast's agglutination state was further evaluated by pretreating the cells with aminoguanidine hydrochloride, as described elsewhere (26).

Statistical analysis. Statistical analyses were performed using GraphPad Prism version 5.00 for Windows (GraphPad Software, San Diego, CA). Unless otherwise noted, a one-way analysis of variance (ANOVA) using a Kruskal-Wallis nonparametric test was used to compare the differences between groups, and individual comparison between groups was done using the Bonferroni posttest. A 95% confidence interval was considered in all experiments. The *t* test was used to compare the numbers of CFU between groups.

RESULTS

MAbs against Hsp60 display different binding constants. Estimated dissociation constant (K_d) values by inhibition ELISA are shown in Table 1. The inhibition experiments show distinct variations among the MAbs that bind to different epitopes on the structure of Hsp60, as determined previously by epitope mapping (11). The lowest K_d values were observed for IgG2a MAbs, followed by those of IgG1 isotypes, whereas the K_d of IgG2b was more than twice as high as that of IgG1 (Table 1; Fig. 1).

Agglutination is dependent on MAb concentration. The different MAbs varied in their capacity to agglutinate *H. capsulatum* yeast cells (Fig. 2D to H). The efficacy was proportional to the binding of the MAbs described by ELISA, with the IgG2a MAbs producing the largest aggregates. ImageJ was used to calculate the sizes of agglutinates observed for each antibody concentration (Fig. 2J), and at least 100 agglutinates were enumerated per condition. We observed that the overall size of the agglutinates was reduced when lower concentrations of MAb were used. For all the MAbs characterized, the 0.075 mg/ml concentration produced the most agglutination. For concentrations of less than 0.075 mg/ml, agglutinate sizes decreased considerably. Yeast agglutination was also assessed by flow cytometry, and the differences estimated by increases/
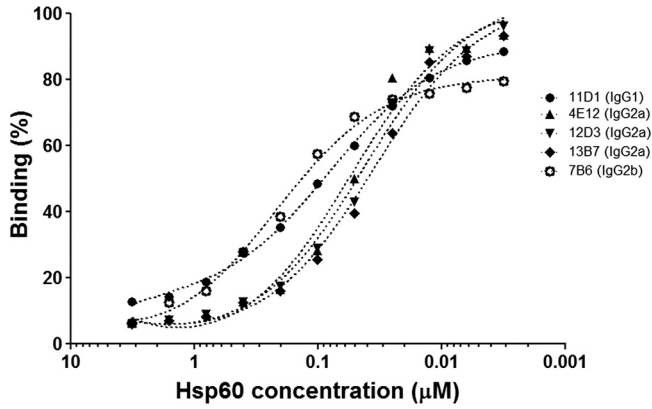
FIG. 1. Inhibition ELISA. The relative saturation is displayed as the function of the concentration of Hsp60. The $Hsp60_{0.5}$ concentration value (the value at which the saturation of total Hsp60 is equal to 50%) can be determined from the curve. Dissociation constant (K_d) values are listed in Table 1.

decreases in forward scatter (FS) values were determined. *H. capsulatum* yeasts incubated with decreasing concentrations of MAb displayed a consistent reduction in the average of agglutinate size of approximately 5 to 10% from the 0.1 to 0.01252 mg/ml concentrations (data not shown) compared to that of untreated yeasts. The agglutination patterns also varied among the antibodies, and agglutination ability decreased with reducing concentrations, displaying similar results to those measured by light microscopy. Clumping sizes comparable to those of the yeast without treatment were observed for nonspecific antibody treatment ($P > 0.05$). These findings suggest that the binding constant and agglutination efficacy are closely associated.

Agglutinates display differences in charge depending on size. *H. capsulatum* yeast cells have a net negative charge in large part due to cell wall glucans (15, 33). In order to characterize the effects of IgGs on the charge of the agglutinates, we examined the effect on zeta potential with one MAb from specific IgG subclasses. *H. capsulatum* yeast incubated with PBS or different concentrations of an irrelevant MAb yielded charges of -30 ± 3 mV. In contrast, increasing concentrations of protective IgG1 or IgG2a reduced the overall charge of
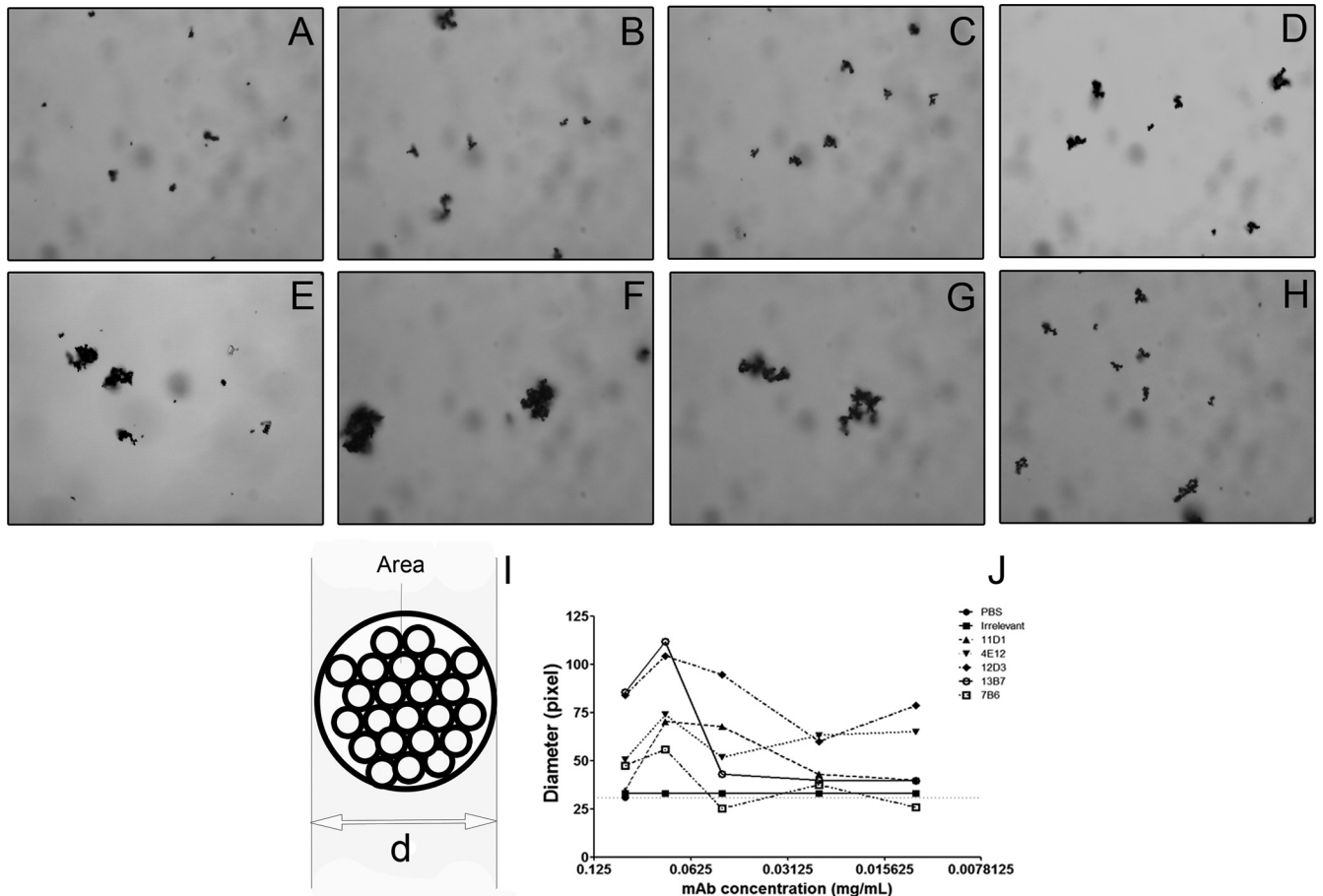

FIG. 2. Agglutination of *H. capsulatum* cells measured by light microscopy and flow cytometry. (A to H) Microscopy of aggregates in which *H. capsulatum* is incubated with water (A), PBS (B), IgG isotype control (C), 11D1 (D), 4E12 (E), 12D3 (F), 13B7 (G), and 7B6 (H). MAb concentration, 0.075 mg/ml. (I) Depiction of the model used for ImageJ calculations of agglutination diameter (d). (J) Light microscopy shows that agglutination is dependent on concentration of MAbs used. Similar results were obtained by flow cytometry (data not shown). The results shown are representative of a minimum of three independent experiments.

TABLE 2. Zeta potentials of agglutinates after incubation with different subclasses and concentrations of MAbs

MAb	Zeta potential at MAb concn (mg/ml)[a]:				
	0.1	0.075	0.050	0.025	0.0125
11D1	−16.19	−16.67	−20.93	−33.08	−20.38
12D3	−18.23	−21.45	−21.56	−30.31	−25.92
7B6	−25.37	−27.63	−18.83	−28.15	−18.82

[a] Values shown are in mV and represent the averages of results from 10 different measurements.

agglutinates (less negative) when increasing antibody concentrations were used, consistent with greater agglutination (Table 2). The nonprotective MAb 7B6 had an inconsistent impact on agglutinate charge.

MAbs display different agglutination kinetics. To further physically evaluate the agglutination properties of antibodies to Hsp60, we coated 85-nm polystyrene beads with a cell wall/membrane extract obtained from *H. capsulatum* yeast and incubated them with different concentrations of the MAbs. Antibodies to Hsp60 induced more agglutination of the coated beads than agglutinates occurring with coated beads incubated with irrelevant MAbs (Table 3), although the agglutination efficacy was extremely varied. It must be noted that the distribution and conformation of an antigen (i.e., Hsp60) on the beads are significantly different than those present on the fungal cell surface, which therefore alters the interactions identified in this experimental system. Nevertheless, this model system confirms that the agglutination effect was due to the binding of MAbs to the antigen, since beads incubated with an irrelevant isotype control MAb displayed values similar to those of untreated beads.

To determine the agglutination efficiency of *H. capsulatum* cells, MAb to Hsp60 or irrelevant controls were used to coat the surfaces of 3-μm carboxyl polystyrene microspheres. The beads coupled with antibody were incubated with FITC-labeled goat anti-mouse IgG and observed by fluorescence microscopy (Fig. 3A to C). The irrelevant and Hsp60-binding MAbs all adhered to the microspheres (Fig. 3A to C), although there was variation in efficacy. Flow cytometric analysis confirmed the microscopy determinations (data not shown). We evaluated the adhesion between MAbs covalently attached to the surfaces of polystyrene microspheres and *H. capsulatum* yeast cells. Agglutinate size was measured by flow cytometry using different bead/cell ratios, and the values were used to determine the slope for the agglutination curve of each MAb (Fig. 3D). The slope represented the binding efficiency, which when normalized by the average amount of MAb present on

the surfaces of the beads correlated with the dissociation constant (K_d) of the MAbs. Using the MAb surface densities determined by flow cytometric (or microscopy) assays and the contact area, we calculated the agglutination efficacy, which was inferred from the agglutinate size measured by flow cytometry, normalized by the proportion of each MAb present on the beads. A correlation was observed when the agglutination efficacy parameter was plotted against the K_d of each MAb obtained by inhibition ELISA (Table 1; Fig. 3E) ($P = 0.045$; Pearson's $r = 0.8867$). The experimental results are consistent with the K_d estimates. Control experiments using only MAb-coated microspheres and uncoated beads processed through the carbodiimide chemistry incubated with the yeast were performed to support that the agglutination observed was due to antibody-antigen binding. No agglutination occurred with the MAb-coated beads in the absence of yeast cells or when uncoated beads were added to suspensions of yeast cells.

Aggregation is dependent on intact MAb structure. Previous work to characterize the protective efficacy of the MAbs against Hsp60 showed that efficacy depended on the MAb subclass and/or the epitope recognized by the MAb (11). We generated Fab′ fragments from protective and disease-enhancing MAbs (12D3 and 7B6, respectively) and assessed whether the fragments differed in their aggregation properties compared to those of the intact MAbs. Fab′ fragments of MAb 12D3 were able to agglutinate *H. capsulatum* yeast but the efficacy was much lower than the intact MAb structure. For both types of Fab fragments, agglutinates were at least 42% smaller than their intact counterparts at equal molar concentrations (data not shown).

Characteristic time indicates additional differences in agglutination activities of the MAbs. Optical tweezers were used to trap washed yeast or yeast incubated with Hsp60 binding or irrelevant MAb. Captured yeast cells were brought into contact with another similarly treated yeast cell using optical tweezers. By monitoring the interactions, we observed binding events in real time. Relative adhesion rates between two *H. capsulatum* yeasts were scored after different interaction times. A plot of the relative adhesion as a function of time revealed that the number of positive attachment events between two *H. capsulatum* yeast cells increased over time (Fig. 4).

The protective MAb 12D3 resulted in 63% yeast-yeast positive adhesion events within τ_{12D3} of 4.5 ± 0.4 s. The characteristic time for the relative adhesion was significantly longer for the nonprotective MAb 7B6 ($P < 0.05$). In this case, 63% yeast-yeast positive adhesion interactions happened within τ_{12D3} of 15 ± 2 s. The characteristic time of the relative adhesion for unopsonized *H. capsulatum* yeast was even more

TABLE 3. Percent increase in size of 85-nm polystyrene-bead agglutinates compared to that of the IgG isotype control

MAb concn (mg/ml)	% size increase[a]				
	11D1	4E12	12D3	13B7	7B6
0.1	48.3 (±10.1)	168.0 (±19.6)	373.1 (±45.8)	308.3 (±39.1)	332.2 (±41.3)
0.075	14.3 (±8.8)	169.0 (±24.9)	238.0 (±32.3)	201.1 (±27.8)	325.0 (±41.4)
0.05	28.8 (±9.9)	263.2 (±34.4)	225.3 (±30.7)	280.7 (±36.6)	286.1 (±37.0)
0.025	40.5 (±9.8)	329.3 (±41.8)	72.9 (±12.8)	195.6 (±27.2)	299.9 (±39.9)
0.0125	165.2 (±19.2)	332.1 (±41.3)	322.3 (±40.4)	398.5 (±48.5)	222.8 (±45.3)

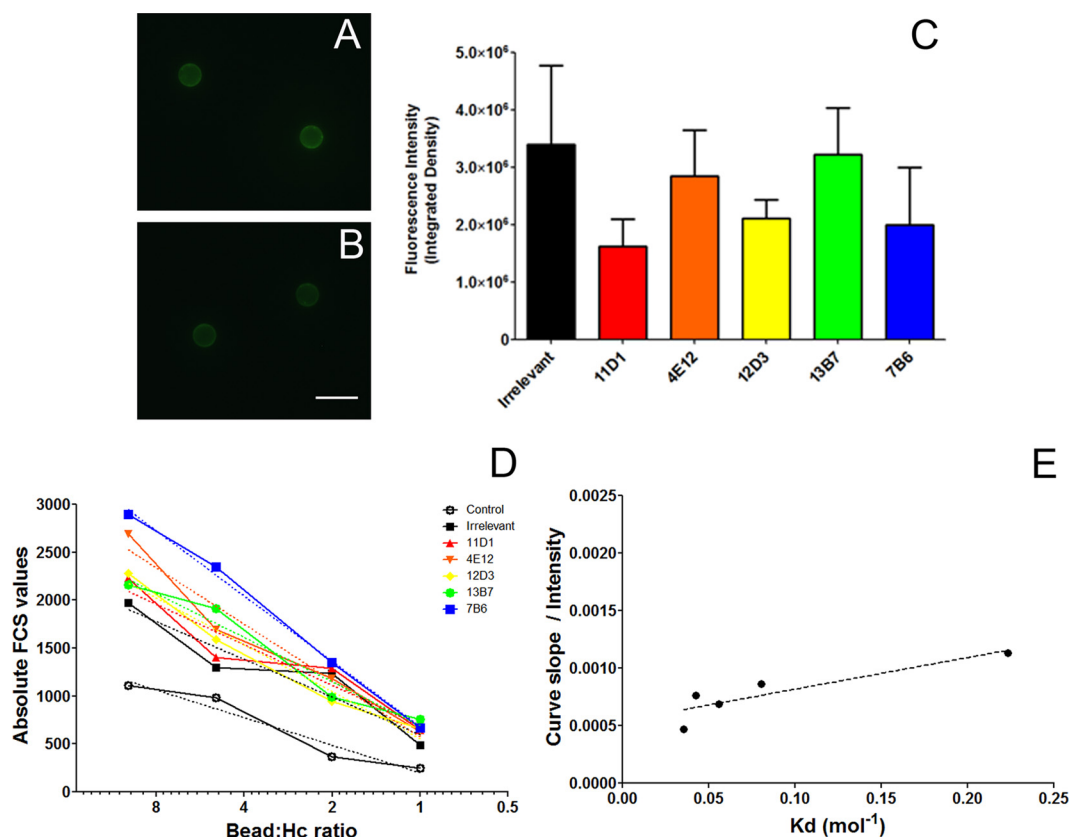[a] Results show the averages from 10 different measurements.

FIG. 3. Characterization of the agglutination efficacy of MAbs by flow cytometry. (A and B) Immunofluorescence of MAb-coupled beads displays an intensity of fluorescence similar to that of the IgG isotype control (A) and MAb 12D3 (B). Fluorescence with MAb 12D3 is representative of the fluorescence produced by incubation with each of the MAbs to Hsp60. Scale bar = 5 μm. (C) Fluorescence intensity of the beads as measured by ImageJ. (D) Agglutination of *H. capsulatum* (Hc) was measured with different bead/yeast ratios, and the slope of the curves is considered the agglutination efficacy. (E) When the slope was normalized by fluorescence intensity on the beads, to calculate the agglutination constant of the MAbs, a correlation with the dissociation constant (K_d) values was observed, obtained by inhibition ELISA. The experiments depicted were repeated three times in duplicate.
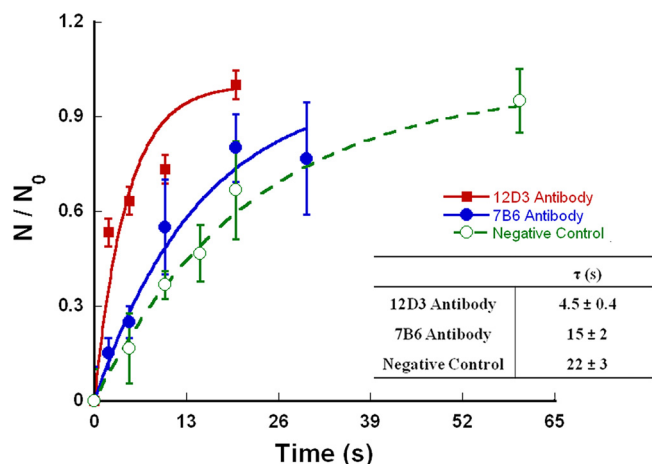

FIG. 4. Relative adhesion as a function of the time intervals during which the opsonized cells were attached using optical tweezers. IgG2a MAb 12D3 displays a lower characteristic time than IgG2b MAb 7B6, followed by the IgG isotype control. These parameters directly correlate with the dissociation constant (K_d) for each MAb. The data shown are averages of results from 3 independent experiments.

protracted than that of the nonprotective MAb 7B6. The characteristic time values measured are in agreement with the binding and agglutination efficacy of the MAbs (Table 1).

Macrophage effector function depends on the agglutination state of *H. capsulatum* yeast. The phagocytosis rates and growth inhibition efficacies of macrophages after agglutination of *H. capsulatum* yeast cells with different MAbs were evaluated. The phagocytosis rates of agglutinates of *H. capsulatum* opsonized with a MAb to Hsp60 increased compared to the values obtained using yeast exposed to an irrelevant control MAb. Figure 5A depicts the phagocytosis rates in the presence of the MAbs to Hsp60 after normalization by the values obtained using an irrelevant control MAb at each concentration. For example, at 50 μg/ml, the phagocytosis rate was 41.2% for PBS and 44.32% for irrelevant controls versus 62.6% for IgG1 11D1, 57.12, 64.14, and 63.1% for IgG2a MAbs 4E12, 12D, and 13B7, respectively, and 66.24% for IgG2b 7B6. As in our prior study, opsonization with MAb 7B6 resulted in the highest rate of phagocytosis (11). For each MAb to Hsp60, the increase in efficacy was concentration dependent, with the highest rates occurring at 0.025 and 0.05 mg/ml. This also suggests that the larger aggregates were less well phagocytosed relative to
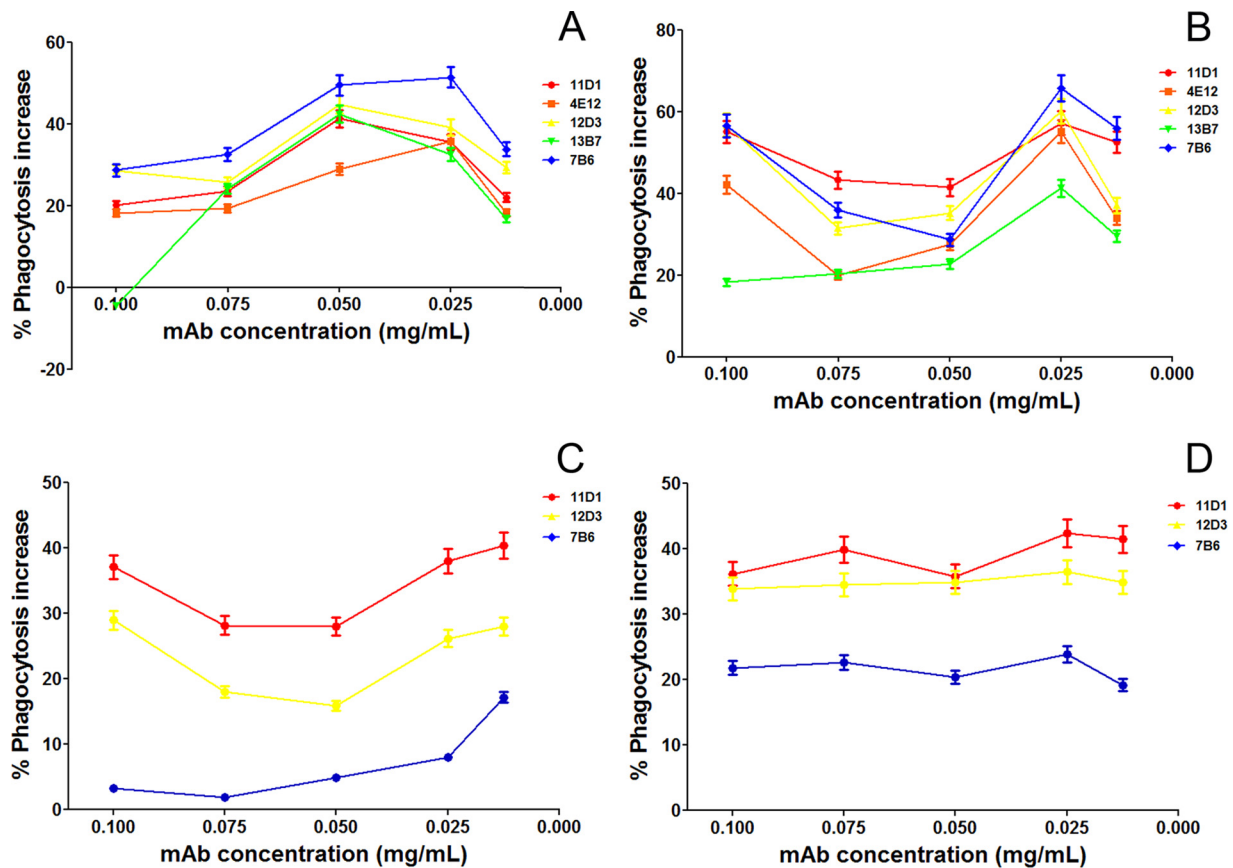
FIG. 5. Phagocytosis of *H. capsulatum* agglutinates by macrophages, normalized by phagocytosis levels obtained with yeast incubated with an isotype control. (A) MAb to Hsp60 increased phagocytosis of *H. capsulatum* yeast, with a greater efficacy for smaller aggregates than larger ones. (B) A blockade of macrophage CR3 receptors reduced the phagocytosis of larger agglutinates compared to that of smaller ones. (C) CD11b$^{-/-}$ macrophages are less able to phagocytose larger agglutinates, and results were similar to those obtained from the CR3 receptor blockage with antibodies. (D) A blockade of Fc receptors reduced the phagocytosis of smaller aggregates compared to that of large ones. The results shown are averages from three independent experiments.

smaller ones. The effect of CR3 was evaluated by a blockade of this receptor with MAbs. Under these conditions, the phagocytosis of larger aggregates was abruptly inhibited, suggesting that aggregates may be more dependent on the presence of available CR3 than individual yeasts. Furthermore, phagocytosis of smaller aggregates was not affected by the CR3 blockade, suggesting that uptake of small aggregates or individual yeasts is occurring through interaction with Fc receptors on the surfaces of macrophage cells (Fig. 5B). These results were confirmed using peritoneal macrophages from CD11b$^{-/-}$ mice in which phagocytosis rates were higher in the presence of smaller aggregates than in the presence of larger ones ($P > 0.05$) (Fig. 5C). With the Fc receptor blockade, we observed an overall decrease in the phagocytosis rates, but there was a more pronounced reduction in the phagocytosis rates of smaller aggregates, resulting in values similar to those of the controls ($P > 0.05$) (Fig. 5D).

Macrophage growth inhibition experiments demonstrated that the effector function of macrophages correlates with aggregation sizes produced by different MAb concentrations. The protective 11D1 (IgG1) and 12D3 (IgG2a) MAbs inhibited the growth of aggregates at concentrations higher than

0.025 mg/ml (Fig. 6A) (P of <0.05 compared to that of controls), and the highest growth restriction was observed at 0.050 mg/ml, which was also the concentration at which there was the highest phagocytosis rate. However, with the disease-enhancing 7B6 MAb, concentrations of ≥ 0.050 mg/ml promoted growth of the aggregates, suggesting a less effective macrophage response (Fig. 6A) ($P < 0.05$). Interestingly, the protective MAbs induced a higher release of nitric oxide by macrophages at MAb concentrations that produced the largest aggregates (Fig. 6B), and nitric oxide generation positively correlated with the agglutination-dependent growth inhibition efficacy of macrophages (Fig. 6C) ($P = 0.05$; $R^2 = 0.18$). However, the disease-enhancing 7B6 MAb maximally induced the release of nitric oxide in the presence of the smallest aggregates examined. The correlation between NO levels and growth inhibition was further confirmed by the use of aminoguanidine hydrochloride, which abrogated the production of macrophage NO in response to agglutinates, resulting in similar fungal growth between the groups assessed (data not shown). Superoxide levels were also measured, and a trend toward higher levels was observed for the protective MAb 12D3 compared to those of nonprotective 7B6, but the values
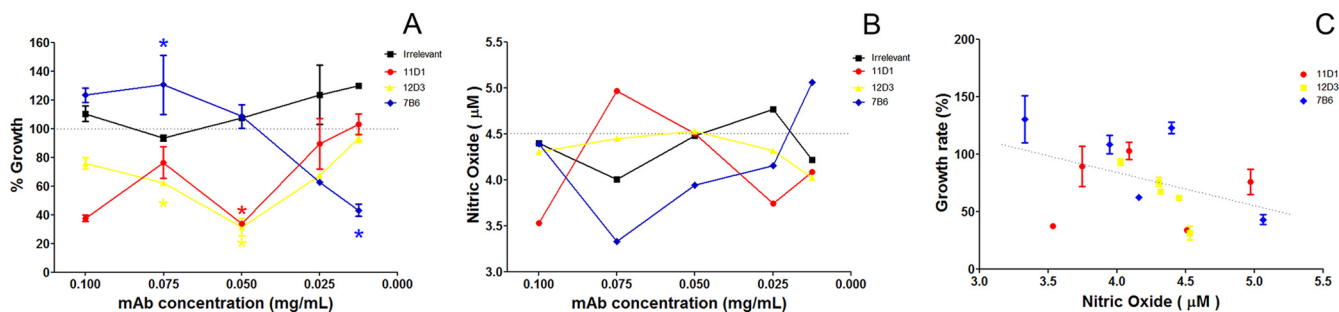
FIG. 6. Effector functions of macrophages are altered depending on the agglutination state of infectious particles. (A) Measurements of *H. capsulatum* growth inhibition by macrophages revealed different outcomes depending on the agglutinate size and the subclass of MAb used ($P < 0.05$). (B) Nitric oxide release by macrophages significantly depended on the agglutinate size and MAb subclass used ($P < 0.05$). The results shown in panels A and B are averages from three independent experiments. (C) Correlation of aggregation-related killing efficacy and nitric oxide levels produced by macrophages show that nitric oxide might be the principal antifungal-related molecule ($P = 0.05$).

did not change among the concentrations tested (data not shown).

DISCUSSION

The therapeutic use of MAbs has emerged as a potential alternative or adjunctive approach to control systemic fungal infections, such as cryptococcosis, candidiasis and histoplasmosis (31, 40). However, the concentration and subclass of MAbs used *in vivo* must be finely determined (40). We previously described IgG MAbs to Hsp60 that varied in their capacity to modify murine histoplasmosis (11). In the course of this work, we noted that the MAbs had a variable capacity to agglutinate yeast cells *in vitro* and that the present studies were designed to more fully characterize this phenomenon.

Opsonization of pathogens by IgGs generally facilitates phagocytosis by effector cells (4, 16, 25). Association of a microorganism opsonized by IgG with a phagocyte typically involves a direct interaction between the antibody and the effector cell via an Fc receptor-mediated process (28, 29). In our *H. capsulatum* models with antibodies to Hsp60, we have shown that increased rates of phagocytosis by the IgG1 and IgG2b subclass MAbs were primarily via Fc receptors, whereas the IgG2a MAbs utilized both Fc and CR3 receptors to augment phagocytosis (11). The involvement of different receptors might also explain the variations in the activation state of macrophages and influence the induction of killing of the phagocytosed pathogen (14, 28).

In the current work, we applied diverse methods to assess the MAb-mediated agglutination of yeast cells, and the results consistently demonstrated that the subclass impacted agglutination efficacy (IgG2a $\gg$ IgG1> IgG2b). Size measurements through microscopy and photometry displayed absolute differences in the particle parameters assessed upon administration of MAb to Hsp60 relative to controls over a range of antibody concentration. Although results were similar with microscopy and flow cytometry, we assumed light microscopy to be the gold standard since this method allowed for recording (image capture) of the particles. Further, microscopy represents the historical standard for characterization of agglutinates in solution (17, 18).

The agglutination efficacy of the MAbs was also measured by assessment of the agglutinate formation rate, as determined by

flow cytometry under conditions in which MAbs were physically trapped on the surfaces of polystyrene beads. Cell-based *in vitro* affinity determination methods provide flexibility, especially for studying MAb binding to cell surface antigens. As MAb-coated beads were titrated into a constant *H. capsulatum* yeast cell concentration, we could determine a slope for the interaction curve generated for each MAb (Fig. 3D). A nonlinear fit of binding measurements corrected by the concentrations of MAbs on each bead (as the total ligand concentration titrated to the cells) showed a correlation with each K_d determination method we tested. This model is therefore applicable to a flow cytometry-based titration analysis for agglutination efficacy, which detects a signal directly proportional to the amount of ligand bound to a cell surface and size (forward side scatter [FCS-H]). The model provides a more accurate description for cell-based titrations than other current methods previously described.

We found that the protective IgG2a MAb 12D3 produced a significantly smaller characteristic time for the relative adhesion and that opsonization with this MAb universally led to cell-cell engagement, which contrasted with cells opsonized with the nonprotective IgG2b MAb 7B6 that displayed a significantly longer characteristic time of association (Fig. 4).

Even though we did not definitively investigate the strength of the antibody-antigen bonds, we were able to correlate the cell-cell interactions (Fig. 4) with dissociation constants from the inhibition ELISAs (Table 1). The binding kinetics showed positive cooperativity with time, and the association rate increased as the number of bonds formed increased. The distribution of times after which the system returned to the unbound state displayed an exponential decay.

Increased avidity of IgGs has been associated with augmented phagocytosis and functional activity against many pathogens (2, 34, 39, 40). Phagocytosis processes by peritoneal macrophages involves a combination of two separate actions, attachment and ingestion (16, 25). Notably, opsonizing IgGs have been characterized that facilitate the attachment phase of phagocytosis in *C. neoformans* (16). The ingestion phase of *C. neoformans* does not require the presence of opsonin (16), and nonspecific interactions are the driving regulators of the ingestion process (30, 43). The current proposed mechanism for the altered rates of phagocytosis of the agglutinated *C. neoformans*

yeasts consists of IgG stabilizing the attachment phase, permitting additional attachment by nonspecific interactions. This model is consistent with results from the bacterium *Enterococcus faecalis*, in which aggregation substance (Asa1) augments adherence and internalization by macrophages with via CD11b/CD18 and agglutinated bacteria survive phagocytosis and inhibit the respiratory burst (37). This is also consistent with our hypothesis for the function of our MAb to *H. capsulatum* Hsp60, in which we propose that the IgGs stabilize or enhance interactions with Fc receptors and/or CR3 integrins (20, 41).

We aimed to correlate the clumping activity of the MAbs with the ability of the cells to adhere to macrophages, since this phenomenon is unclear for *H. capsulatum*/macrophage interactions, although it suggests that aggregation by MAbs alters phagocytosis. Flow cytometry analyses revealed that large agglutinates are phagocytosed less efficiently than small aggregates and single cells in the presence of MAbs as opsonins. A blockade of CR3 of J774 macrophages or the use of CD1b$^{-/-}$ peritoneal macrophages resulted in an additional reduction in the phagocytosis of larger aggregates, confirming that CR3 nonspecific interactions are involved in the phagocytosis of the large agglutinates. Further, we demonstrated that the blockade of the Fc receptor decreased the overall phagocytosis rates but with more pronounced reduction in the phagocytosis of smaller aggregates, suggesting the importance of Fc receptors in the phagocytosis of smaller opsonized particles.

The fungicidal activity of the macrophages for *H. capsulatum* yeast cells in the presence of the different MAb concentrations varied according to subclass and aggregation state of the infectious particles. Considering that different subclasses of MAbs have distinct affinity for the different Fcγ receptors, the MAbs could also be differentially activating (or inhibiting) the fungicidal responses of the macrophages. IgG1 and IgG2a MAbs can interact strongly with Fcγ receptor I (FcγRI) and FcγRIII (29), facilitating the induction of phagocytosis and activation of the respiratory burst, enhancing growth inhibition or killing. However, IgG2b MAbs interact strongly with FcγRIV and FcγRIIB, which are activation and inhibitory Fc receptors, respectively. Activation through FcγRIV *in vivo* is associated with lung inflammation (22). In contrast, FcγRIIB is involved in the inhibition of macrophage microbicidal responses. Our data fit with this information, since we have shown that IgG1s and IgG2as are protective and that ingestion of *H. capsulatum* opsonized with these MAbs facilitates macrophage killing, while macrophages are permissive to *H. capsulatum* growth when the yeast cells are opsonized by IgG2b MAb 7B6.

When the *H. capsulatum*-containing macrophage populations were analyzed after yeast cell opsonization with MAbs, we observed a higher number of yeast cells per phagocytic cell relative to control conditions. This is consistent with our prior studies (11). However, in the present work, we examined the levels of nitric oxide and found that they were significantly higher in supernatants of macrophages that ingested larger agglutinates, since phagocytosis of large agglutinates is dependent on the CR3 and Fc receptors, and entry into the macrophages through this pathway induces the respiratory burst. This is also consistent with the hypothesis that internalization of yeast by macrophage strictly via CR3 inhibits the respiratory

burst (5, 36, 47). These findings are also supported by our recent observation that IgG2b levels were significantly increased in histoplasmosis in mice treated with methamphetamine, and these mice have accelerated disease and increased mortality (24). Hence, certain antibodies may be detrimental, especially compromising the capacity of macrophages to combat this intracellular invader. However, it is unclear if naturally occurring nonspecific agglutination of *H. capsulatum* yeasts might facilitate agglutination and impact intracellular survival. Notably, new techniques for the isolation of different cell clusters sizes have to be developed in order to characterize this potential effect.

Our observations of MAbs against *H. capsulatum* Hsp60 reveal an additional mechanism for regulating fungal phagocytosis rates and macrophage effector functions. These findings contribute to the elucidation of the role of IgGs as a mediator of immune defense. They also provide us with valuable information that can be translated into an *in vivo* histoplasmosis model, which could lead to insights into the development of robust antibody responses to vaccines or the selection of MAb doses for prophylactic or therapeutic purposes. Although the biological relevance of agglutination of *H. capsulatum* yeasts during infection remains unclear, given that the fungus is largely intracellular, clusters of extracellular yeast have been clearly documented in murine (32) and human (19, 35, 46) disease. Presumably, these aggregates are either extruded cells from a lysed phagocyte or locally proliferated yeasts that are held together by cell-cell interactions facilitated by host factors, including antibody. In either case, these fungal cells are accessible to antibody. Further study will be required to define the biology of yeast agglutination *in vivo*. Interestingly, we recently correlated macrophage effector functions to aggregation caused by opsonins in a *Streptococcus pneumoniae* model using an IgM MAb to capsular polysaccharide (6). Hence, the role of MAb-induced agglutination may have broad import in additional pathogens.

REFERENCES

1. **Allendoerfer, R., G. P. Biovin, and G. S. Deepe, Jr.** 1997. Modulation of immune responses in murine pulmonary histoplasmosis. J. Infect. Dis. **175:**905–914.
2. **Bachmann, M. F., et al.** 1997. The role of antibody concentration and avidity in antiviral protection. Science **276:**2024–2027.
3. **Bialek, R., et al.** 2002. Comparison of staining methods and a nested PCR assay to detect Histoplasma capsulatum in tissue sections. Am. J. Clin. Pathol. **117:**597–603.
4. **Diamond, R. D., J. E. May, M. A. Kane, M. M. Frank, and J. E. Bennett.** 1974. The role of the classical and alternate complement pathways in host defenses against Cryptococcus neoformans infection. J. Immunol. **112:**2260–2270.

5. **Eissenberg, L. G., and W. E. Goldman.** 1987. Histoplasma capsulatum fails to trigger release of superoxide from macrophages. Infect. Immun. **55:**29–34.

6. **Fabrizio, K., C. Manix, A. J. Guimaraes, J. D. Nosanchuk, and L.-A. Pirofski.** 2010. Aggregation of *Streptococcus pneumoniae* by a pneumococcal capsular polysaccharide specific human monoclonal IgM correlates with antibody efficacy *in vivo*. Clin. Vaccine Immunol. **17:**713–721.

7. **Fasching, C. E., et al.** 2007. Impact of the molecular form of immunoglobulin A on functional activity in defense against Streptococcus pneumoniae. Infect. Immun. **75:**1801–1810.

8. **Gomez, A. M., J. C. Rhodes, and G. S. Deepe, Jr.** 1991. Antigenicity and immunogenicity of an extract from the cell wall and cell membrane of Histoplasma capsulatum yeast cells. Infect. Immun. **59:**330–336.

9. **Goodwin, R. A., J. E. Loyd, and R. M. Des Prez.** 1981. Histoplasmosis in normal hosts. Medicine (Baltimore) **60:**231–266.

10. **Guimaraes, A. J., et al.** 2010. Evaluation of an enzyme linked immunosorbent assay (ELISA) using purified, deglycosylated histoplasmin for different clinical manifestations of Histoplasmosis. Microbiol. Res. **2:**e1.

11. **Guimaraes, A. J., S. Frases, F. J. Gomez, R. M. Zancope-Oliveira, and J. D. Nosanchuk.** 2009. Monoclonal antibodies to heat shock protein 60 alter the pathogenesis of Histoplasma capsulatum. Infect. Immun. **77:**1357–1367.

12. **Guimaraes, A. J., A. J. Hamilton, H. L. de M. Geudes, J. D. Nosanchuk, and R. M. Zancope-Oliveira.** 2008. Biological function and molecular mapping of M antigen in yeast phase of Histoplasma capsulatum. PLoS One **3:**e3449.

13. **Habich, C., et al.** 2006. Heat shock protein 60: identification of specific epitopes for binding to primary macrophages. FEBS Lett. **580:**115–120.

14. **Kaneko, Y., F. Nimmerjahn, and J. V. Ravetch.** 2006. Anti-inflammatory activity of immunoglobulin G resulting from Fc sialylation. Science **313:**670–673.

15. **Klimpel, K. R., and W. E. Goldman.** 1988. Cell walls from avirulent variants of Histoplasma capsulatum lack alpha-(1,3)-glucan. Infect. Immun. **56:**2997–3000.

16. **Kozel, T. R., and T. G. McGaw.** 1979. Opsonization of Cryptococcus neoformans by human immunoglobulin G: role of immunoglobulin G in phagocytosis by macrophages. Infect. Immun. **25:**255–261.

17. **Latimer, P.** 1975. The influence of photometer design on optical-conformational changes. J. Theor. Biol. **51:**1–12.

18. **Latimer, P., D. M. Moore, and F. D. Bryant.** 1968. Changes in total light scattering and absorption caused by changes in particle conformation. J. Theor. Biol. **21:**348–367.

19. **Levy, A. D., J. C. Shaw, and L. H. Sobin.** 2009. Secondary tumors and tumorlike lesions of the peritoneal cavity: imaging features with pathologic correlation. Radiographics **29:**347–373.

20. **Long, K. H., F. J. Gomez, R. E. Morris, and S. L. Newman.** 2003. Identification of heat shock protein 60 as the ligand on Histoplasma capsulatum that mediates binding to CD18 receptors on human macrophages. J. Immunol. **170:**487–494.

21. **Macura, N., T. Zhang, and A. Casadevall.** 2007. Dependence of macrophage phagocytic efficacy on antibody concentration. Infect. Immun. **75:**1904–1915.

22. **Mancardi, D. A., et al.** 2008. FcgammaRIV is a mouse IgE receptor that resembles macrophage FcepsilonRI in humans and promotes IgE-induced lung inflammation. J. Clin. Invest. **118:**3738–3750.

23. **Maresca, B., and G. S. Kobayashi.** 1989. Dimorphism in Histoplasma capsulatum: a model for the study of cell differentiation in pathogenic fungi. Microbiol. Rev. **53:**186–209.

24. **Martinez, L. R., M. R. Mihu, A. Gacser, L. Santambrogio, and J. D. Nosanchuk.** 2009. Methamphetamine enhances histoplasmosis by immunosuppression of the host. J. Infect. Dis. **200:**131–141.

25. **McGaw, T. G., and T. R. Kozel.** 1979. Opsonization of Cryptococcus neoformans by human immunoglobulin G: masking of immunoglobulin G by cryptococcal polysaccharide. Infect. Immun. **25:**262–267.

26. **Miles, P. R., L. Bowman, A. Rengasamy, and L. Huffman.** 1998. Constitutive nitric oxide production by rat alveolar macrophages. Am. J. Physiol. **274:**L360–L368.

27. **Mukherjee, S., M. Feldmesser, and A. Casadevall.** 1996. J774 murine macrophage-like cell interactions with Cryptococcus neoformans in the presence and absence of opsonins. J. Infect. Dis. **173:**1222–1231.

28. **Nimmerjahn, F., P. Bruhns, K. Horiuchi, and J. V. Ravetch.** 2005. FcgammaRIV: a novel FcR with distinct IgG subclass specificity. Immunity **23:**41–51.

29. **Nimmerjahn, F., and J. V. Ravetch.** 2005. Divergent immunoglobulin g subclass activity through selective Fc receptor binding. Science **310:**1510–1512.

30. **Nir, S., and M. Andersen.** 1977. Van der Waals interactions between cell surfaces. J. Membr. Biol. **31:**1–18.

31. **Nosanchuk, J. D.** 2005. Protective antibodies and endemic dimorphic fungi. Curr. Mol. Med. **5:**435–442.

32. **Nosanchuk, J. D., J. N. Steenbergen, L. Shi, G. S. Deepe, Jr., and A. Casadevall.** 2003. Antibodies to a cell surface histone-like protein protect against Histoplasma capsulatum. J. Clin. Invest. **112:**1164–1175.

33. **Rappleye, C. A., J. T. Engle, and W. E. Goldman.** 2004. RNA interference in Histoplasma capsulatum demonstrates a role for alpha-(1,3)-glucan in virulence. Mol. Microbiol. **53:**153–165.

34. **Romero-Steiner, S., et al.** 1999. Reduction in functional antibody activity against Streptococcus pneumoniae in vaccinated elderly individuals highly correlates with decreased IgG antibody avidity. Clin. Infect. Dis. **29:**281–288.

35. **Schwarz, J., E. Bingham, E. S. Robbins, and S. M. Adriano.** 1955. Experimental histoplasmosis in mice, and pregnancy. J. Infect. Dis. **97:**160–161.

36. **Shi, L., et al.** 2008. A monoclonal antibody to Histoplasma capsulatum alters the intracellular fate of the fungus in murine macrophages. Eukaryot. Cell **7:**1109–1117.

37. **Sussmuth, S. D., et al.** 2000. Aggregation substance promotes adherence, phagocytosis, and intracellular survival of Enterococcus faecalis within human macrophages and suppresses respiratory burst. Infect. Immun. **68:**4900–4906.

38. **Svoboda, K., and S. M. Block.** 1994. Biological applications of optical forces. Annu. Rev. Biophys. Biomol. Struct. **23:**247–285.

39. **Taborda, C. P., and A. Casadevall.** 2002. CR3 (CD11b/CD18) and CR4 (CD11c/CD18) are involved in complement-independent antibody-mediated phagocytosis of Cryptococcus neoformans. Immunity **16:**791–802.

40. **Taborda, C. P., J. Rivera, O. Zaragoza, and A. Casadevall.** 2003. More is not necessarily better: prozone-like effects in passive immunization with IgG. J. Immunol. **170:**3621–3630.

41. **Vanek, N. N., et al.** 1999. Enterococcus faecalis aggregation substance promotes opsonin-independent binding to human neutrophils via a complement receptor type 3-mediated mechanism. FEMS Immunol. Med. Microbiol. **26:**49–60.

42. **Viana, N. B., M. S. Rocha, O. N. Mesquita, A. Mazolli, P. A. Maia Neto, and H. M. Nussenzveig.** 2007. Towards absolute calibration of optical tweezers. Phys. Rev. E. Stat. Nonlin. Soft Matter Phys. **75:**021914.

43. **Weir, D. M., and H. M. Ogmundsdottir.** 1977. Non-specific recognition mechanisms by mononuclear phagocytes. Clin. Exp. Immunol. **30:**323–329.

44. **Wheat, J.** 1997. Histoplasmosis. Experience during outbreaks in Indianapolis and review of the literature. Medicine (Baltimore) **76:**339–354.

45. **Wheat, L. J., and C. A. Kauffman.** 2003. Histoplasmosis. Infect. Dis. Clin. North Am. **17:**1–19.

46. **Whitt, S. P., G. A. Koch, B. Fender, N. Ratnasamy, and E. D. Everett.** 2004. Histoplasmosis in pregnancy: case series and report of transplacental transmission. Arch. Intern. Med. **164:**454–458.

47. **Wolf, J. E., V. Kerchberger, G. S. Kobayashi, and J. R. Little.** 1987. Modulation of the macrophage oxidative burst by Histoplasma capsulatum. J. Immunol. **138:**582–586.

48. **Woods, J. P.** 2003. Knocking on the right door and making a comfortable home: Histoplasma capsulatum intracellular pathogenesis. Curr. Opin. Microbiol. **6:**327–331.

49. **Zugel, U., and S. H. Kaufmann.** 1999. Immune response against heat shock proteins in infectious diseases. Immunobiology **201:**22–35.